

Title

Salicylic acid induces mitochondrial injury by inhibiting ferrochelatase heme biosynthesis activity

Authors

Vipul Gupta, Shujie Liu, Hideki Ando, Ryohei Ishii, Shumpei Tateno, Yuki Kaneko, Masato Yugami, Satoshi Sakamoto, Yuki Yamaguchi, Osamu Nureki, and Hiroshi Handa

Affiliations

Department of Biological Information, Graduate School of Bioscience and Biotechnology, Tokyo Institute of Technology, 4259 Nagatsuta-cho, Midori-ku, Yokohama 226-8501, Japan (V.G., S.L., H.A., S.T., Y.K., M.Y., S.S., Y.Y., H.H.)

Department of Biophysics and Biochemistry, Graduate School of Science, the University of Tokyo, 2-11-16 Yayoi, Bunkyo-ku, Tokyo 113-0032, Japan (R.I., O.N.)

Running Title

Ferrochelatase is a novel target of salicylic acid

Corresponding Author

Hiroshi Handa

Tokyo Institute of Technology

4259 Nagatsuta-cho, Midori-ku, Yokohama 226-8501, Japan

Phone: +81-45-924-5872, Fax: +81-45-924-5145

E-mail: handa.h.aa@m.titech.ac.jp

Number of text pages: 38

Number of tables: 1

Number of Figures: 5

Number of references: 49

Number of words in the Abstract: 236

Number of words in the Introduction: 584

Number of words in the Discussion: 883

Abbreviations

AMPK, adenosine monophosphate-activated protein kinase; COX, cyclooxygenase;
FCCP, carbonyl cyanide *p*-trifluoromethoxyphenylhydrazone; FECH, ferrochelatase;
FG beads, ferrite-glycidyl methacrylate affinity beads; GST, glutathione S-transferase;
His, histidine; *m*-HBA, *meta*-hydroxybenzoic acid; NF- κ B, nuclear factor kappa B;
PpIX, protoporphyrin IX; *p*-HBA, *para*-hydroxybenzoic acid; SA, salicylic acid; SDS,
sodium dodecyl sulfate; UPLC, ultra-high performance liquid chromatography;
Zn-PpIX, zinc-protoporphyrin IX.

Abstract

Salicylic acid is a classic non-steroidal anti-inflammatory drug. Although salicylic acid also induces mitochondrial injury, the mechanism of its anti-mitochondrial activity is not well understood. In this study, by using a one-step affinity purification scheme with salicylic acid-immobilized beads, ferrochelatase (FECH), a homodimeric enzyme involved in heme biosynthesis in mitochondria, was identified as a new molecular target of salicylic acid. Moreover, co-crystal structure of the FECH•salicylic acid complex was determined. Structural and biochemical studies showed that salicylic acid binds to the dimer interface of FECH in two possible orientations and inhibits its enzymatic activity. Mutational analysis confirmed that Trp301 and Leu311, hydrophobic amino acid residues located at the dimer interface, are directly involved in salicylic acid binding. On a gel filtration column, salicylic acid caused a shift in the elution profile of FECH, indicating that its conformational change is induced by salicylic acid binding. In cultured human cells, salicylic acid treatment or FECH knockdown inhibited heme synthesis, whereas salicylic acid did not exert its inhibitory effect in FECH knockdown cells. Concordantly, salicylic acid treatment or FECH knockdown inhibited heme synthesis in zebrafish embryos. Strikingly, the salicylic acid-induced effect in zebrafish was partially rescued by FECH overexpression. Taken together, these findings illustrate that FECH is responsible for salicylic acid-induced inhibition of heme synthesis, which may contribute to its anti-mitochondrial and anti-inflammatory function. This study establishes a novel aspect of the complex pharmacological effects of salicylic acid.

Introduction

The therapeutic effect of willow bark, of which the active ingredient is now known to be salicylic acid, was first reported about 3500 years ago in Egyptian manuscripts (Nicolaou and Montagnon, 2008). Originally recognized as an anti-pathogen plant hormone (Durner et al., 1997), the drug was later chemically synthesized by Kolbe (Needs and Brooks, 1985), leading to the development of the salicylic acid family of non-steroidal anti-inflammatory drugs. The most popular member of this family is aspirin or acetyl salicylic acid, which is rapidly hydrolyzed to salicylic acid by plasma esterase after administration (Grosser et al., 2009). In addition to analgesia, aspirin and salicylic acid can cause various adverse events, such as gastrointestinal toxicity, renal toxicity, hepatic injury, and neurological and respiratory imbalances (Grosser et al., 2009; Needs and Brooks, 1985).

The anti-inflammatory effect of aspirin is generally thought to be caused by the inhibition of cyclooxygenase (COX) activity during prostaglandin biosynthesis (Vane, 1971; Vane and Botting, 2003). Unlike aspirin, salicylic acid has almost no inhibitory activity against purified COX, but nevertheless inhibits prostaglandin synthesis in intact cells (Mitchell et al., 1993). This suggests that other targets might account for the anti-inflammatory actions of salicylic acid. Indeed, I κ B kinase β (IKK- β), a key enzyme in the nuclear factor (NF)- κ B pathway, is inhibited by aspirin and salicylic acid (Kopp and Ghosh, 1994; Yin et al., 1998); however, the actions of salicylic acid are still observed in NF- κ B p105-deficient mice (Cronstein et al., 1999; Langenbach et al., 1999), suggesting that it has yet another target. Recently, adenosine monophosphate-activated protein kinase (AMPK) was identified as a new target of salicylic acid (Hawley et al., 2012). Salicylic acid, but not aspirin, allosterically activates AMPK, thereby increasing fat metabolism (Hawley et al., 2012). Nonetheless, the possible link between this finding and the anti-inflammatory function

of salicylic acid remains unknown.

Several reports have shown that salicylic acid causes mitochondrial injury, resulting in an inhibition of ATP synthesis, mitochondrial swelling, and the disruption of mitochondrial membrane potential (Braun et al., 2012; Doi and Horie, 2010; Klampfer et al., 1999). The mitochondrial damage may contribute to the anti-inflammatory actions of salicylic acid, possibly by reducing cellular ATP levels and promoting the release of adenosine (Cronstein et al., 1999), an autocoid with strong anti-inflammatory properties (Cronstein, 1994). To better understand the mechanism of action of drugs such as salicylic acid, we previously developed high performance affinity beads that allow one-step affinity purification of drug target proteins from crude cell extracts (Sakamoto et al., 2009). By using this methodology, we successfully identified new molecular targets of pharmacological drugs and elucidated novel cellular mechanisms responsible for their actions (Ito et al., 2010; Sakamoto et al., 2009; Shimizu et al., 2000; Uga et al., 2006). In the present work, this technology was used to identify ferrochelatase (FECH, EC 4.99.1.1) as a novel target of salicylic acid that is involved in its mitochondrial actions.

FECH is a ubiquitously expressed, inner mitochondrial membrane protein of the heme biosynthesis pathway that catalyzes the insertion of ferrous ions into protoporphyrin IX (PpIX) to form heme. Heme serves as the prosthetic group of various hemoproteins that are vital for cell viability, such as oxygen-carrying hemoglobin and myoglobin and energy-producing cytochromes in the electron transport chain (Atamna et al., 2001; Atamna et al., 2002; Gatta et al., 2009; Möbius et al., 2010). We now show that salicylic acid inhibits FECH-catalyzed heme synthesis *in vitro* and *in vivo*. This inhibition is likely to be responsible, at least in part, for salicylic acid-induced mitochondrial injury.

Materials and Methods

Cell culture, antibodies, and reagents. K562 cells were cultured in RPMI 1640 medium supplemented with 10% fetal bovine serum. 293T cells were cultured in DMEM supplemented with 10% fetal bovine serum. To knock down human FECH, the following sequences were used as a target of shRNA: sh#1, 5'-CCAAGGGGTGTGGAGTTGGAA-3'; sh#2, 5'-GACCATATTGAAACGCTGTAT-3'. Lentiviral vectors expressing these shRNAs were produced and infected into 293T cells, followed by selection with puromycin for a few days. The resulting cells were then used for subsequent analyses.

Rabbit polyclonal antibody against FECH was obtained from Abcam. Sodium salicylate was dissolved in ultrapure water, buffer, or directly in medium, as appropriate. Stock solutions of *meta*-hydroxybenzoic acid (*m*-HBA) and *para*-hydroxybenzoic acid (*p*-HBA) were prepared in 1 M NaOH, and the pH was adjusted to 7.4. Stock solutions of PpIX (10 mM in dimethyl sulfoxide, Frontier Scientific) and zinc acetate (10 mM in milliQ) were prepared and stored at -20°C until use.

Preparation of salicylic acid-immobilized beads and affinity purification.

Salicylic acid was immobilized on carboxylated ferrite-glycidyl methacrylate (FG) beads by using 200 mM *N*-hydroxysuccinimide and 200 mM 1-ethyl-3-(3-dimethylaminopropyl)-carbodiimide. Beads were then incubated with 30 mM 5-amino salicylic acid (Nacalai Tesque) in *N,N*-dimethylformamide for 24 h at room temperature. Unreacted carboxylic acids were masked with 1 M 2-ethanolamine in *N,N*-dimethylformamide, and the resulting beads were stored at 4°C until use (Supplemental Figure 1B). For affinity purification, salicylic acid-immobilized beads (0.2 mg) were equilibrated with buffer IB-A (20 mM HEPES [pH 7.9], 100 mM KCl,

0.1% Triton X-100, 10% glycerol). Extracts were prepared from K562 cells, Jurkat cells, rat liver mitochondria, or rat brain mitochondria in buffer IB-A. The extracts were incubated with the salicylic acid-immobilized beads for 2 h at 4°C. The beads were washed with buffer IB-A, and bound proteins were eluted with SDS-containing sample buffer. In some experiments, salicylic acid was added to the extracts prior to incubation with the beads.

Expression and purification of recombinant FECH. The R115L variant of full-length human FECH was inserted into pGEX-6P-1 (GE Healthcare). The plasmid was further modified so that N-terminally truncated His-tagged FECH R115L was expressed under the control of the *tac* promoter. Essentially the same construct was used for expression and crystallization of FECH (Burden et al., 1999).

Cell-free FECH enzymatic assay. Enzymatic activity was measured as the amount of Zn-PpIX produced by aerobic incorporation of zinc into PpIX by recombinant FECH, as described previously (Li et al., 1987). Briefly, all reactions were performed in buffer IB-C (250 mM Tris-HCl, pH 8.2, 1% TritonX-100, and 1.75 mM palmitic acid). Buffer IB-C containing purified recombinant FECH R115L or another mutant (1 µg) with or without salicylic acid, *m*-HBA, or *p*-HBA was first incubated for 1 h at 4°C and then for 5 min at 25°C. After the addition of PpIX and zinc acetate to the final concentration of 10 µM for each reagent, the reaction (250 µl) was further incubated for 5 min, terminated by the addition of dimethyl sulfoxide:methanol mixture (750 µl; 30:70 v/v), and centrifuged at 7000 rpm for 10 min. The supernatant was filtered through 0.22 µm centrifugal filter (Millipore), and the filtrate was applied to a Waters 600 HPLC system equipped with a 4.6 × 150 mm 5C₁₈–AR-II column (Nacalai Tesque) or to an Acquity UPLC system (Waters) equipped with a 2.1 × 50 mm C₁₈ column (Waters,

186002350). The sample was resolved with a linear gradient of ammonium acetate/methanol that ranged from 0.25 M ammonium acetate (pH 5.16)/75% methanol to 0.05 M ammonium acetate (pH 5.16)/95% methanol. Zn-PpIX and PpIX were monitored by the absorbance at 416 and 400 nm, respectively. Their identities were confirmed by applying a mixture of commercially available Zn-PpIX and PpIX as the standard to the column.

Crystallization, data collection, and structure determination. For the crystallization of the R115L FECH•salicylic acid (FECH•SA) complex, purified FECH R115L (500 μ M) was incubated with 10 mM sodium salicylate for 1 h at 4°C. Crystals were obtained by using polyethylene glycol as a precipitant. Red crystals of the FECH•SA complex were obtained by incubating the protein-salicylic acid mixture (200 nl) with 0.1 M PCB buffer (200 nl; pH 4.8) containing 10% PEG1500 at 20°C for 3 days (Supplemental Figure 3C). For cryoprotection, the crystals were soaked in a reservoir solution containing 25% ethylene glycol. X-ray diffraction data were collected at the SPring-8 beamline BL41XU facility (wavelength 1.0 Å, temperature 100 K, Japan Synchrotron Radiation Research Institute, Hyogo, Japan) and processed with HKL2000 software (Otwinowski and Minor, 1997). Other crystallographic calculations were performed with the CCP4 package package (Collaborative Computational Project, 1994). The structure of the FECH•SA complex was determined via the molecular replacement method, based on the structure of the apoenzyme (PDB code: 2HRC) (Medlock et al., 2007b) as a search model with Molrep. Model building was accomplished with Coot (Emsley and Cowtan, 2004), and refinement was performed by using REFMAC5 (Steiner et al., 2003) and Phenix (Afonine et al., 2012). Data collection and structure refinement statistics are summarized in Supplemental Table 1. The Ramachandran statistics were 97.8/2.2/0

(%), corresponding to favored/allowed/outliers. The atomic coordinates for the R115L FECH-salicylic acid complex structure have been deposited in the Protein Data Bank, www.pdb.org (PDB ID code 3W1W).

Gel filtration. Gel filtration was performed by using an AKTA explorer (GE Healthcare) equipped with a Superdex 200 10/300 column (GE Healthcare). For Figure 2F, FECH R115L (4 mg/ml) or FECH R115L/L311A (3 mg/ml) was first incubated with the indicated concentration of salicylic acid for 1 h at 4°C. Then, 100 µl of the sample was loaded onto the column using buffer IB-B (50 mM Tris-MOPS [pH 8.0], 100 mM KCl, 1.0% (w/v) sodium cholate, 250 mM imidazole) containing the same concentration of salicylic acid as column buffer. Eluate fractions (500 µl each) were collected, and peak fractions were analyzed by SDS-PAGE and Coomassie Brilliant Blue staining. The column was calibrated with the protein markers (GE Healthcare) aldolase (158 kDa), ovalbumin (44 kDa), and ribonuclease-A (13.7 kDa).

Quantification of cellular heme content. Total heme was extracted and analyzed by ultra-high performance liquid chromatography (UPLC), essentially as described previously (Antonicka et al., 2003). K562 or 293T cells (2×10^6) were seeded onto six-well plates and then incubated with different concentrations of salicylic acid, *m*-HBA, or *p*-HBA for 24 h at 37°C. After washing with phosphate buffered saline (PBS), cells were lysed by the sequential addition of acetone/conc. HCl/water (175 µl; 77.5: 2.5: 20) and 50% acetonitrile (200 µl) with vigorous shaking. After centrifugation at $20,400 \times g$ for 10 min at 4°C, the supernatant (200 µl) was collected and filtered through a 0.22 µm centrifugal filter (Millipore). The pH of the sample was adjusted to ~3–4 by the addition of NH₄OH, and the sample was applied to UPLC system equipped with 2.1 × 50 mm C₁₈ column (Waters). Heme was eluted at a flow rate of

0.2 ml/min by using a 30–50% acetonitrile gradient for the first minute, followed by a 50–95% acetonitrile gradient for the next 9 min. All column buffers contained 0.05% trifluoroacetic acid. The elution of heme was monitored by measuring the absorbance at 400 nm. The retention time of heme was confirmed by using commercially available hemin as the control (Frontier Scientific).

Quantification of NAD(P)H content. NAD(P)H content in cells was quantified by using the WST-8 assay (Nacalai Tesque). The assay is based on the extracellular reduction of WST-8 by NAD(P)H produced in the mitochondria (Berridge et al., 2005). K562 cells were seeded into 96-well plates at 5,000 cells/50 μ l/well. Salicylic acid, *m*-HBA, or *p*-HBA (50 μ l/well) was added to each well, and after 24 h of incubation at 37°C, WST-8 was added. The absorbance at 450 nm was determined by using a plate reader (Wallac 1420 ARVO SX). Data were reported as the percentage of the absorbance in untreated controls.

Mitochondrial membrane potential. Flow cytometry was used for the determination of mitochondrial membrane potential (MMP, $\Delta\Psi$). K562 cells were seeded into six-well dishes at 1×10^6 cells/ml/well. Salicylic acid, *m*-HBA, *p*-HBA (10 mM), or FCCP (10 μ M; Sigma) was added (in 1 ml of the same medium) and incubated for 24 or 48 h. Cells were stained with 10 μ M Rhodamine 123 (Sigma) for 15 min at 37°C, washed with PBS, and analyzed with a FACScalibur (Becton-Dickinson).

Zebrafish experiments. Zebrafish embryos (1 hpf); dechorionated by using 2 mg/ml protease type XIV (Sigma), were immersed in salicylic acid (0.5, 1, or 3 mM in E3 medium) for 47 h, as described previously (Ito et al., 2010). Knockdown and rescue experiments were performed by microinjecting an antisense morpholino

oligonucleotide (1 to 2 ng) targeting *zFECH* (5'-CACGCGCCTCCTAAAACCGCCATTG-3'), with or without capped mRNA for *zFECH* (0.6 ng; Gene Tools, Philomath, OR, USA), as described previously (Ito et al., 2010). Heme was visualized by *o*-dianisidine staining of 48 hpf embryos, as described previously (Ransom et al., 1996). Accumulation of PpIX in living 48-hpf embryos was detected by fluorescence microscopy using its autofluorescence with illumination peak at 520-550 nm (Childs et al., 2000).

Results

Salicylic acid binds to FECH. To identify novel salicylic acid-binding proteins, FG beads were used (Sakamoto et al., 2009). An amino derivative of salicylic acid (Supplemental Figure 1A) was conjugated to carboxylated FG beads (Supplemental Figure 1B). K562 human erythroleukemia cell lysate was preincubated with different concentrations of free salicylic acid and then incubated with the salicylic acid-immobilized beads. After extensive washing, bound proteins were eluted by using sodium dodecyl sulfate (SDS)-containing sample buffer and then subjected to SDS-polyacrylamide gel electrophoresis (SDS-PAGE) and silver staining. A polypeptide with an apparent molecular weight of ~40 kDa (Figure 1A, top, arrow) was associated with the salicylic acid-immobilized beads, and its binding was inhibited by increasing concentrations of free salicylic acid (Figure 1A, top). Because none of the known targets of salicylic acid has a similar molecular weight, this protein was subjected to proteolytic digestion and tandem mass spectrometry. The protein was finally identified as FECH, an inner mitochondrial membrane protein involved in the heme biosynthesis pathway. The identity of FECH was further confirmed by immunoblotting analysis with an antibody against human FECH (Figure 1A, bottom). In addition, the use of different protein sources such as Jurkat cells (an immortalized T lymphocyte cell line), rat liver mitochondria, and rat brain mitochondria confirmed the association of FECH with salicylic acid-immobilized beads (Supplemental Figures 2A and 2B). Thus, salicylic acid binds to FECH in a species- or cell type-independent manner.

Salicylic acid inhibits FECH activity. Because of its high expression and ready purification, we used the processed form of human FECH carrying an R115L substitution for most of the subsequent experiments. Although the Arg115 residue

makes a contact with the physiological substrate of FECH, PpIX, the R115L mutant and the wild-type enzyme share similar catalytic activity (Medlock et al., 2007b). However, the R115L mutant is considerably more stable *in vitro* (Burden et al., 1999; Wu et al., 2001). We found that the binding efficiency of His-FECH R115L to salicylic acid beads was indistinguishable from that of wild-type FECH fused to glutathione-S-transferase (GST) (compare Figure 1B and Supplemental Figure 2C). Because FECH can employ Zn^{2+} as a substrate (Li et al., 1987; Medlock et al., 2007b), the formation of a Zn-PpIX complex from Zn^{2+} and PpIX was examined *in vitro* by using purified recombinant FECH R115L. As expected, salicylic acid inhibited its enzymatic activity in a concentration-dependent manner (Figure 1D).

To gain insight into the functional importance of the above findings, we next performed structure-function analysis with free *ortho*-hydroxybenzoic acid (salicylic acid), *meta*-hydroxybenzoic acid (*m*-HBA), and *para*-hydroxybenzoic acid (*p*-HBA) (Supplemental Figure 1A). To our knowledge, only a single study has compared the pharmacological actions of these three isomers (You, 1983). This previous study showed that salicylic acid, but not its isomers, caused the swelling of rat liver mitochondria. Similarly, we found that free salicylic acid inhibited the association of FECH with salicylic acid-immobilized beads more efficiently than free *m*-HBA or free *p*-HBA (Figure 1C). Moreover, *m*-HBA and *p*-HBA had little effect on FECH activity in the same concentration range as salicylic acid (Figure 1D). These data indicate that salicylic acid specifically binds to FECH and inhibits its enzymatic activity.

In severe cases of rheumatic fever and rheumatoid arthritis, high doses of aspirin are administered, resulting in its metabolite, salicylic acid, increasing to concentrations of 1–3 mM in the plasma and above 4 mM in the tissue (Baggott et al., 1992). To obtain quantitative data on the FECH-salicylic acid interaction, isothermal titration calorimetry was used. The dissociation constant of this interaction was in the

range of 5–15 mM (Supplemental Figure 4), which is similar to or slightly higher than pharmacologically relevant concentrations of salicylic acid. All of the *in vitro* binding and enzymatic assays performed in this study included Triton X-100 to prevent the aggregation of FECH and the non-enzymatic formation of Zn-PpIX. At a high concentration, however, Triton X-100 is clearly inhibitory to the interaction of FECH with salicylic acid (Supplemental Figure 2D), suggesting that the presence of the detergent underlies the weak affinity of salicylic acid for FECH *in vitro*. It may be that a certain fraction of the salicylic acid is entrapped in the micelle in the presence of Triton X-100, and is thus unable to interact with FECH.

Salicylic acid binds to the dimer interface of FECH. The crystal structures of human FECH, either in free form or complexed with PpIX, have been reported (Dailey et al., 2007; Medlock et al., 2007a, 2007b, 2009, 2012; Wu et al., 2001). To determine the structural basis for the interaction between FECH and salicylic acid, the co-crystal structure of the FECH•SA complex was determined at a resolution of 2.0 Å (Figure 2A). Each asymmetric unit of the structure consists of two FECH molecules forming a dimer, with the dimer interface situated on the non-crystallographic axis. Consistent with previous studies, a [2Fe-2S] cluster was found attached to each FECH protomer covalently through Cys196, Cys403, Cys406, and Cys411. In addition, one ethylene glycol molecule, five cholate molecules, and 417 water molecules were found in each asymmetric unit (Supplemental Figure 7). The overall structure of FECH•SA is essentially the same as the previously reported structure for the apoenzyme form of FECH (Wu et al., 2001; Medlock et al., 2007b). There is a clear electron density that is well fitted to a single molecule of salicylic acid between the two FECH protomers at the two-fold axis (Figure 2B). It is possible to model salicylic acid in two opposite orientations (Figure 2C), and the average B-factors of salicylic acid are 16.7 Å² and

17.9 Å², respectively. The two structures are essentially identical, and salicylic acid is surrounded by hydrophobic amino acids such as Val270, Pro277, Trp301, and Leu311 originating from both protomers (Figures 2B and 2C). The hydroxyl group of salicylic acid forms a hydrogen bond with the side chain of Ser281 at a distance of 2.7 or 2.8 Å (Figures 2B and 2C). These residues form a dimer interface channel (Medlock et al., 2012), and salicylic acid sits in the middle of the channel.

To test the validity of our structural data and to examine the amino acid residues of FECH important for its binding to salicylic acid, Val270, Ser281, Trp301, and Leu311 were mutated to alanine, and a binding assay was performed by using salicylic acid-immobilized beads and FECH R115L mutants. Figure 2D shows that the W301A (R115L/W301A) and L311A (R115L/L311A) point mutations, but not the S281A (R115L/S281A) point mutation, substantially reduced FECH binding to salicylic acid. The V270A (R115L/V270A) mutant bound to salicylic acid, albeit to a lesser extent than FECH R115L. These results suggest that the hydrogen bond between the hydroxyl group of salicylic acid and FECH Ser281 is dispensable and that the hydrophobic interactions of the benzene ring of salicylic acid with FECH Trp301 and Leu311 are critical to salicylic acid binding to the dimer interface.

Because the amino acid residues studied above are located at the dimer interface, it is possible that some of the point mutations inhibit salicylic acid binding indirectly by affecting the dimerization status of FECH. Gel filtration analysis was performed to test this hypothesis. While FECH R115L and R115L/S281A were eluted with an estimated molecular weight of ~90 kDa, R115L/V270A, R115L/W301A, and R115L/L311A were eluted with an estimated molecular weight of ~50 kDa (Supplemental Figure 3A), suggesting that these mutants exist largely as monomers (summarized in Table 1). Because the monomeric mutant R115L/V270A retained significant salicylic acid-binding activity (Figure 2D), we concluded that the

dimerization of FECH is not required for its interaction with salicylic acid. Incidentally, none of the monomeric mutants we identified showed detectable enzymatic activity (Table 1), in agreement with earlier studies demonstrating that the dimerization of FECH is essential for its function (Wu et al., 2001; Medlock et al., 2007b; Najahi-Missaoui and Dailey, 2005). To investigate whether the amino acid residues Trp301 and Leu311 are directly involved in salicylic acid binding, we analyzed these mutants in the monomeric background. As expected, an additional W301A or L311A mutation to R115L/V270A resulted in the loss of salicylic acid binding (Figure 2D). These results are consistent with our structural data and together demonstrate that Trp301 and Leu311 of FECH are directly involved in its binding to salicylic acid.

Monomeric bacterial FECH also binds to salicylic acid. FECH is widely conserved across species, and bacterial homologs of FECH are known to function as monomers (Wu et al., 2001). This prompted us to investigate whether bacterial FECH also binds to salicylic acid. As a result, we found that recombinant FECH derived from *Escherichia coli* bound to salicylic acid to the same extent as the human monomeric R115L/V270A FECH mutant (Figure 2E). Concordantly, amino acid residues critical for salicylic acid binding are conserved between mammalian and bacterial FECHs (Supplemental Figure 6). The above finding strengthens our conclusion that the dimerization of FECH is not required for salicylic acid binding.

Salicylic acid induces conformational changes in FECH. Since salicylic acid binds to the dimer interface of FECH, we next investigated the possibility that salicylic acid affects the dimerization status of FECH. For this purpose, gel filtration analysis was performed in the presence of different concentrations of salicylic acid. As shown in Figure 2F, the presence of salicylic acid clearly shifted the elution peak of FECH

R115L but had little effect on the elution profile of FECH R115L/L311A, a monomeric mutant defective in salicylic acid binding. By contrast, *p*-HBA did not appreciably affect the elution profile of FECH R115L (Supplemental Figure 3B), suggesting that the shift is specific and is mediated by salicylic acid binding to FECH. However, the shift was not as dramatic as that caused by the R115L/L311A mutation (Figure 2F), indicating that salicylic acid may cause a conformational change in the dimer rather than its complete dissociation. This finding apparently contradicts our structural data, which did not reveal any conformational change in FECH upon salicylic acid binding. One explanation might be that the crystal structure we obtained only represents an initial binding state. Regardless, the salicylic acid-induced structural change, evidenced by gel filtration analysis, may be related to its inhibitory effect on FECH's enzymatic activity.

Salicylic acid inhibits heme synthesis and mitochondrial activity in K562 cells.

We next investigated the effect of salicylic acid on cellular heme biosynthesis by using UPLC. As shown in Figure 3A, salicylic acid treatment for 24 h resulted in a substantial reduction in the heme content of K562 cells, with a maximum decrease of $64\pm3\%$ observed at 10 mM. The effects of *m*-HBA and *p*-HBA were comparatively weak, with maximum decreases of $16\pm2\%$ and $15\pm4\%$, respectively, at 10 mM. Hence, salicylic acid, but not *m*-HBA and *p*-HBA, inhibits FECH activity both in cell-free assays and K562 cells.

Next, salicylic acid-induced mitochondrial injuries were investigated in two different assays: (i) WST-8 (tetrazolium salt) assay, which measures NAD(P)H and hence general mitochondrial energy metabolism, and (ii) Rhodamine 123 assay, which measures mitochondrial membrane potential by using a fluorescent lipophilic cationic dye. As determined by the WST-8 assay, salicylic acid resulted in a

significant dose-dependent decrease in cellular NAD(P)H levels, with an IC_{50} of ~3 mM after 24 h incubation (Figure 3B). By contrast, *m*-HBA and *p*-HBA had only a modest inhibitory effect. In the Rhodamine 123 assay, K562 cells were incubated for 24 or 48 h with salicylic acid, *m*-HBA, or *p*-HBA (10 mM of each), or with the uncoupler carbonyl cyanide *p*-trifluoromethoxyphenylhydrazone (FCCP, employed as the positive control). At 24 h, only a small, if any, reduction in membrane potential was induced under any of the conditions examined (Figure 3C). At 48 h, salicylic acid yielded a 52% decrease in fluorescence, which was comparable to that induced by FCCP (Figure 3C). By contrast, *m*-HBA and *p*-HBA had only a modest effect on membrane potential. Collectively, these results reveal that salicylic acid, but not *m*-HBA and *p*-HBA, inhibits the synthesis of heme and NAD(P)H in K562 cells and impairs mitochondrial membrane potential. While similar findings have already been reported for salicylic acid (Braun et al., 2012; Klampfer et al., 1999), this is, to our knowledge, the first comparative study of salicylic acid and its isomers.

FECH is responsible for the inhibitory effect of salicylic acid on heme synthesis.

To investigate the functional link between FECH and salicylic acid more critically, we knocked down FECH in 293T cells by transducing lentiviral vectors expressing one of two shRNAs against FECH (Figure 4A). Then, the cellular levels of heme was measured with or without prior incubation with 1, 3 and 10 mM of salicylic acid. FECH knockdown alone resulted in a reduction of the cellular heme level (data not shown). Moreover, FECH knockdown abolished salicylic acid-induced reduction of the heme level at all concentration of salicylic acid (Figure 4B), suggesting that FECH is responsible for the inhibitory effect of salicylic acid on heme synthesis, and mediating some of its pharmacological effects.

Salicylic acid inhibits heme synthesis and accumulates PpIX in zebrafish. To

extend our findings to the whole animal level, we next used zebrafish embryos as an experimental model. Amino acid sequences of human and zebrafish FECH (zFECH) are 79% identical, and moreover, several amino acid residues important for salicylic acid binding are conserved between the species (Supplemental Figure 6). We first investigated whether zFECH binds to salicylic acid and found that zFECH binds to salicylic acid-immobilized beads as efficiently as human FECH (Supplemental Figure 2C).

We next analyzed the effect of salicylic acid on heme synthesis during zebrafish development by *o*-dianisidine staining of heme. In control 48 h post-fertilization (hpf) embryos, hematocytes in the blood sinus covering the yolk were stained in a granular pattern (Figure 5A). A small embryo-to-embryo variation was observed in *o*-dianisidine staining, probably due to the different running patterns of the blood sinus. While *zFECH*-knockdown (*zFECH* antisense morpholino oligonucleotide) or salicylic acid-treated embryos showed no gross morphological abnormalities (Supplemental Figure 5), *o*-dianisidine staining was generally decreased in these embryos (Figure 5B). The spectrum of embryonic phenotypes was divided into “strong,” “intermediate”, and “weak” categories, based on the staining intensity and the diagnostic criteria shown in Figure 5A. While almost all of the *zFECH*-knockdown embryos showed a reduction in heme biosynthesis, co-injection of *zFECH* mRNA partially restored production of heme (Figure 5B). Similarly, salicylic acid (1 or 3 mM) strongly inhibited heme generation in a concentration-dependent manner (Figure 5B), in agreement with our findings *in vitro* and in cultured cells. Remarkably, overexpression of zFECH in salicylic acid-treated embryos partially restored heme production (Figure 5C). By contrast, *m*-HBA and *p*-HBA had no significant effect on heme production in zebrafish (Figure 5D).

If the defect in heme synthesis is indeed due to the inhibition of FECH, its substrate PpIX may be conversely accumulated in affected embryos. Hence, PpIX auto-fluorescence in zebrafish embryos was examined under a fluorescence microscope at an illumination peak of 520-550 nm. As expected, zFECH knockdown embryos showed a substantial accumulation of PpIX in the blood sinus covering the yolk, and this accumulation was reversed by simultaneous overexpression of zFECH (Figure 5E). Similarly, salicylic acid-treated embryos showed a substantial increase in the PpIX level. Thus, these results indicate that salicylic acid inhibits heme biosynthesis by inhibiting FECH activity during zebrafish development.

Discussion

This study found that FECH is a novel salicylic acid-binding protein. FECH is an inner mitochondrial, homodimeric protein that faces the matrix side, contains a (2Fe-2S) cluster, and is involved in the heme biosynthesis pathway (Wu et al., 2001). Several lines of evidence support the idea that salicylic acid decreases heme biosynthesis by inhibiting FECH: (i) FECH binds to salicylic acid-immobilized beads (Figure 1A); (ii) salicylic acid inhibits the enzymatic activity of recombinant FECH *in vitro* (Figure 1D); (iii) salicylic acid binds to FECH at the dimer interface, which is thought to be critical for its activity (Figures 2A–C); (iv) salicylic acid decreases heme content in cultured human cells, and its inhibitory effect is abrogated by the knockdown of FECH (Figures 3 and 4); (v) salicylic acid inhibits heme synthesis in zebrafish, which can be partially rescued by the overexpression of zFECH (Figure 5); and (vi) salicylic acid isomers (*m*-HBA and *p*-HBA) are less effective than salicylic acid in all the assays examined.

How does FECH discriminate salicylic acid from its isomers? Salicylic acid is known to have higher lipid solubility than *m*-HBA and *p*-HBA (Kunze et al., 1972). This occurs because the negative charge of the carboxylate of salicylic acid is delocalized through intramolecular hydrogen bonding between the carboxyl group and the hydroxyl group. Thus, salicylate may move into the hydrophobic dimer interface of FECH more easily than *meta*- or *para*-hydroxybenzoate. Another possibility may be that the hydrogen bond between the hydroxyl group of salicylic acid and FECH Ser281 contributes to isoform specificity. However, this idea is not consistent with our mutational analysis showing that the hydrogen bond is dispensable for their interaction (Figure 2D). Yet another possibility is that the hydroxyl group of *m*-HBA and *p*-HBA causes steric hindrance with surrounding FECH molecules. However, this possibility was not supported by molecular modeling of *m*-HBA and *p*-HBA complexed with FECH. As to the question of how salicylic acid inhibits FECH activity, the

negative charge of salicylic acid may cause conformational changes in the FECH dimer interface and thereby inhibit its enzymatic activity.

Here we showed that salicylic acid affects heme content, NAD(P)H content, and mitochondrial membrane potential at millimolar concentrations in K562 cells. Similarly, previous studies showed that salicylic acid inhibits oxidative phosphorylation and decreases the ATP:AMP ratio at similar concentrations (Cronstein et al., 1999). These consequences can result from the inhibition of FECH because its inhibition should result in the loss of activity of heme proteins, such as cytochromes, that are essential for the generation of mitochondrial membrane potential and ATP synthesis, among others (Atamna et al., 2001; Atamna et al., 2002; Gatta et al., 2009; Möbius et al., 2010). It is also possible that other known targets of salicylic acid (*e.g.*, COX, AMPK, and IKK- β) are involved in the mitochondrial dysfunction. In regard to COX, salicylic acid has little, if any, effect on the enzymatic activity of purified COX (Mitchell et al., 1993). Thus, it seems unlikely that COX plays a role in the salicylic acid-induced mitochondrial dysfunction. In regard to AMPK, salicylic acid is known to activate the essential regulator of energy metabolism (Hawley et al., 2012). This should result in an increase in ATP synthesis; in fact, however, salicylic acid inhibited mitochondrial ATP synthesis (Cronstein et al., 1999). Therefore, the AMPK pathway does not seem to be involved in the salicylic acid-induced mitochondrial injury. In regard to IKK- β , salicylic acid inhibits its protein kinase activity and attenuates inflammatory and immune responses involving NF- κ B (Kopp and Ghosh, 1994; Yin et al., 1998). Since NF- κ B is a crucial regulator of cellular energy metabolism (Mauro et al., 2011), its inhibition by salicylic acid can affect mitochondrial energy metabolism. Hence, the mitochondrial dysfunction induced by salicylic acid may be due to a combination of inhibitory actions on FECH and the NF- κ B pathway.

Although highly speculative, the present findings may have relevance to the anti-inflammatory actions of salicylic acid. Aspirin (acetyl salicylic acid) inhibits COX by transferring its acetyl group to the active site of prostaglandin synthase (Loll et al., 1995). Despite the absence of the acetyl group and no significant effect on purified COX, salicylic acid has similar anti-inflammatory effects *in vivo* and can inhibit COX activity in cell-based assays (Mitchell et al., 1993). A few explanations have been proposed as to how salicylic acid might mitigate inflammation. For example, salicylic acid might inhibit the NF- κ B pathway, which controls the expression of the COX-2 gene (Lim et al., 2001). Because heme is the prosthetic group of COX (Chen et al., 1989), our findings suggest that salicylic acid may inhibit COX indirectly by blocking FECH activity and heme synthesis. Another possible explanation for the anti-inflammatory actions of salicylic acid is that it induces the release of cellular adenosine, an endogenous anti-inflammatory agent that acts on adenosine A2 receptors (Cronstein, 1994). A previous study showed that salicylic acid attenuates inflammation by an adenosine-dependent mechanism, even in mice lacking COX-2 or the p105 subunit of NF- κ B (Cronstein et al., 1999), leading to the idea that there may be an additional target of salicylic acid. This target may be FECH, given that the inhibition of heme synthesis and the resultant inhibition of ATP synthesis might trigger the accumulation of adenosine and its release. Our findings therefore provide new insight into the mechanism behind the complex pharmacological effects of this compound.

Acknowledgments

We thank the Material Analysis Suzukake-dai Center (Technical Department, Tokyo Institute of Technology) for heme analysis, and the staff at the SPring-8 beamline BL41XU facility for assistance in data collection.

Author Contributions

Participated in research design: Gupta, Ando, Ishii, Nureki, Handa.

Conducted experiments: Gupta, Liu, Ando, Ishii.

Contributed new reagents and analytic tools: Tateno, Kaneko, Yugami, Sakamoto.

Performed data analysis: Gupta, Ando, Ishii, Yamaguchi.

Wrote or contributed to writing of the manuscript: Gupta, Yamaguchi.

References

Afonine PV, Grosse-Kunstleve RW, Echols N, Headd JJ, Moriarty NW, Mustyakimov M, Terwilliger TC, Urzhumtsev A, Zwart PH, and Adams, PD (2012) Towards automated crystallographic structure refinement with phenix.refine. *Acta Crystallogr D Biol Crystallogr* **68**:352-367.

Antonicka H, Mattman A, Carlson CG, Glerum DM, Hoffbuhr KC, Leary SC, Kennaway NG, Shoubridge EA (2003) Mutations in COX15 produce a defect in the mitochondrial heme biosynthetic pathway, causing early-onset fatal hypertrophic cardiomyopathy. *Am J Hum Genet* **72**:101-114.

Atamna H, Killilea DW, Killilea AN, Ames BN (2002) Heme deficiency may be a factor in the mitochondrial and neuronal decay of aging. *Proc Natl Acad Sci* **99**:14807-14812.

Atamna H, Liu J and Ames BN (2001) Heme deficiency selectively interrupts assembly of mitochondrial complex IV in human fibroblasts: relevance to aging. *J Biol Chem* **276**:48410-48416.

Baggott JE, Morgan SL, Ha T, Vaughn WH, Hine RJ (1992) Inhibition of folate-dependent enzymes by non-steroidal anti-inflammatory drugs. *Biochem J* **282**:197-202.

Berridge MV, Herst PM, Tan AS (2005) Tetrazolium dyes as tools in cell biology: new insights into their cellular reduction. *Biotechnol Annu Rev* **11**:127-152.

Braun FK, Al-Yacoub N, Plötz M, Möbs M, Sterry W, Eberle J (2012) Nonsteroidal anti-inflammatory drugs induce apoptosis in cutaneous t-cell lymphoma cells and enhance their sensitivity for TNF-related apoptosis-inducing ligand. *J Invest Dermatol* **132**: 429-439.

Burden AE, Wu C, Dailey TA, Busch JL, Dhawan IK, Rose JP, Wang B, Dailey HA (1999) Human ferrochelatase: crystallization, characterization of the (2Fe-2S) cluster and determination that the enzyme is a homodimer. *Biochim Biophys Acta* **1435**:191-197.

Chen YN, and Marnett LJ (1989) Heme prosthetic group required for acetylation of prostaglandin H synthase by aspirin. *FASEB J* **3**:2294-2297.

Childs S, Weinstein BM, Mohideen MA, Donohue S, Bonkovsky H, Fishman MC. (2000) Zebrafish dracula encodes ferrochelatase and its mutation provides a model for erythropoietic protoporphyria. *Curr Biol.* **10**:1001-1004.

Collaborative Computational Project, Number 4 (1994) The CCP4 suite: programs for protein crystallography. *Acta Crystallogr D Biol Crystallogr* **50**:760-763.

Cronstein BN (1994) Adenosine, an endogenous anti-inflammatory agent. *J Appl Physiol* **76**:5-13.

Cronstein BN, Montesinos MC, and Weissmann G (1999) Salicylates and sulfasalazine, but not glucocorticoids, inhibit leukocyte accumulation by an adenosine-dependent mechanism that is independent of inhibition of

prostaglandin synthesis and p105 of NFkappaB. *Proc Natl Acad Sci* **96**:6377-6381.

Dailey HA, Wu CK, Horanyi P, Medlock AE, Najahi-Missaoui W, Burden AE, Dailey TA, Rose J (2007) Altered orientation of active site residues in variants of human ferrochelatase. Evidence for a hydrogen bond network involved in catalysis. *Biochemistry* **46**:7973-7979.

Doi H, and Horie T (2010) Salicylic acid-induced hepatotoxicity triggered by oxidative stress. *Chem Biol Interact* **183**:363-368.

Durner J, Shah J, and Klessig DF (1997) Salicylic acid and disease resistance in plants. *Trends Plant Sci* **2**:266-274.

Emsley P, and Cowtan K (2004) Coot: model-building tools for molecular graphics. *Acta Crystallogr D Biol Crystallogr* **60**:2126-2132.

Gatta LB, Vitali M, Verardi R, Arosio P, Finazzi D (2009) Inhibition of heme synthesis alters amyloid precursor protein processing. *J Neural Transm* **116**:79-88.

Grosser T, Emer S, and Garret AFD (2009) Anti-Inflammatory, Antipyretic, and Analgesic Agents; Pharmacotherapy of Gout, in *The Pharmacological Basis of Therapeutics* (Brunton LL, Chabner BA, Knollmann BC eds) pp 959-1004, Goodman & Gilman's.

Hawley SA, Fullerton MD, Ross FA, Schertzer JD, Chevtzoff C, Walker KJ, Pegg MW, Zibrova D, Green KA, Mustard KJ, Kemp BE, Sakamoto K, Steinberg GR, Hardie DG (2012) The ancient drug salicylate directly activates AMP-activated protein kinase. *Science* **336**:918-922.

Ito T, Ando H, Suzuki T, Ogura T, Hotta K, Imamura Y, Yamaguchi Y, Handa H (2010) Identification of a primary target of thalidomide teratogenicity. *Science* **327**:1345-1350.

Klampfer L, Cammenga J, Wisniewski HG, and Nimer SD (1999) Sodium salicylate activates caspases and induces apoptosis of myeloid leukemia cell lines. *Blood* **93**:2386-2394.

Kopp E, and Ghosh S (1994) Inhibition of NF-kappa B by sodium salicylate and aspirin. *Science* **265**:956-959.

Kunze H, Rehbock G, Vogt W (1972) Absorption of salicylic acid and its isomers from the rat jejunum. *Naunyn Schmiedebergs Arch Pharmacol* **273**:331-40.

Langenbach R, Loftin CD, Lee C, and Tiano H (1999) Cyclooxygenase-deficient mice. A summary of their characteristics and susceptibilities to inflammation and carcinogenesis. *Ann N Y Acad Sci* **889**:52-61.

Li FM, Lim CK, and Peters TJ (1987) An HPLC assay for rat liver ferrochelatase activity. *Biomed Chromatogr* **2**:164-168.

Lim JW, Kim H, and Kim KH (2001) Nuclear factor-kappaB regulates cyclooxygenase-2 expression and cell proliferation in human gastric cancer cells. *Lab Invest* **81**:349-360.

Loll PJ, Picot D, and Garavito RM (1995) The structural basis of aspirin activity inferred from the crystal structure of inactivated prostaglandin H2 synthase. *Nat Struct Biol* **2**:637-643.

Mauro C, Leow SC, Anso E, Rocha S, Thotakura AK, Tornatore L, Moretti M, De Smaele E, Beg AA, Tergaonkar V, Chandel NS, Franzoso G (2011) NF-kB controls energy homeostasis and metabolic adaptation by upregulating mitochondrial respiration. *Nat Cell Biol* **13**:1272-1279.

Medlock AE, Dailey TA, Ross TA, Dailey HA, and Lanzilotta WN (2007a) A pi-helix switch selective for porphyrin deprotonation and product release in human ferrochelatase. *J Mol Biol* **373**:1006-1016.

Medlock A, Swartz L, Dailey TA, Dailey HA, Lanzilotta WN (2007b) Substrate interactions with human ferrochelatase. *Proc Natl Acad Sci* **104**:1789-1793.

Medlock AE, Carter M, Dailey TA, Dailey HA, Lanzilotta WN (2009) Product release rather than chelation determines metal specificity for ferrochelatase. *J Mol Biol* **393**:308-319.

Medlock AE, Najahi-Missaoui W, Ross TA, Dailey TA, Burch J, O'Brien JR, Lanzilotta WN, Dailey HA (2012) Identification and characterization of solvent-filled channels in human ferrochelatase. *Biochemistry* **51**:5422-5433.

Mitchell JA, Akarasereenont P, Thiemermann C, Flower RJ, and Vane JR (1993) Selectivity of nonsteroidal anti-inflammatory drugs as inhibitors of constitutive and inducible cyclooxygenase. *Proc Natl Acad Sci* **90**:11693-11697.

Möbius K, Arias-Cartin R, Breckau D, Hännig AL, Riedmann K, Biedendieck R, Schröder S, Becher D, Magalon A, Moser J, Jahn M, Jahn D (2010) Heme biosynthesis is coupled to electron transport chains for energy generation. *Proc Natl Acad Sci* **107**:10436-10441.

Najahi-Missaoui W, and Dailey HA (2005) Production and characterization of erythropoietic protoporphyrin heterodimeric ferrochelatases. *Blood* **106**:1098-1104.

Needs CJ, and Brooks PM (1985) Clinical Pharmacokinetics of the salicylate. *Clin Pharmacokinet* **10**:64-177.

Nicolaou KC, and Montagnon T (2008) Molecules That Changed the World, Weinheim: WILEY-VCH.

Otwinowski Z, and Minor W (1997) Processing of x-ray diffraction data collected in oscillation mode. *Methods Enzymol* **276**:307-326.

Ransom DG, Haffter P, Odenthal J, Brownlie A, Vogelsang E, Kelsh RN, Brand M, van Eeden FJ, Furutani-Seiki M, Granato M, Hammerschmidt M, Heisenberg CP, Jiang YJ, Kane DA, Mullins MC, Nüsslein-Volhard C (1996) Characterization of zebrafish mutants with defects in embryonic hematopoiesis. *Development* **123**:311-319.

Sakamoto S, Kabe Y, Hatakeyama M, Yamaguchi Y and Handa H (2009) Development and application of high-performance affinity beads: toward chemical biology and drug discovery. *Chem Rec* **9**:66-85.

Shimizu N, Sugimoto K, Tang J, Nishi T, Sato I, Hiramoto M, Aizawa S, Hatakeyama M, Ohba R, Hatori H, Yoshikawa T, Suzuki F, Oomori A, Tanaka H, Kawaguchi H, Watanabe H, Handa H (2000) High-performance affinity beads for identifying drug receptors. *Nat Biotechnol* **18**:877-881.

Steiner RA, Lebedev AA, and Murshudov GN (2003) Fisher's information in maximum-likelihood crystallographic refinement. *Acta Crystallogr D Biol Crystallogr* **59**:2114-2124.

Uga H, Kuramori C, Ohta A, Tsuboi Y, Tanaka H, Hatakeyama M, Yamaguchi Y, Takahashi T, Kizaki M, and Handa H (2006) A new mechanism of methotrexate action revealed by target screening with affinity beads. *Mol Pharmacol* **70**:1832-1839.

Vane JR, and Botting RM (2003) The mechanism of action of aspirin. *Thromb Res* **110**:255-258.

Vane JR (1971) Inhibition of prostaglandin synthesis as a mechanism of action for aspirin-like drugs. *Nat New Biol* **231**:232-235.

Wu CK, Dailey HA, Rose JP, Burden A, Sellers VM, and Wang BC (2001) The 2.0 Å structure of human ferrochelatase, the terminal enzyme of heme biosynthesis. *Nat Struct Biol* **8**:156-160.

Yin MJ, Yamamoto Y, and Gaynor RB (1998) The anti-inflammatory agents aspirin and salicylate inhibit the activity of I(kappa)B kinase-beta. *Nature* **396**:77-80.

You K (1983) Salicylate and mitochondrial injury in reye's syndrome. *Science* **221**:163-165.

Footnotes

This work was partially supported by a Grant-in-Aid for Scientific Research on Innovative Areas titled “Chemical Biology of Natural Products” from the Ministry of Education, Culture, Sports, Science and Technology (MEXT) of Japan; a Grant-in-Aid for Scientific Research on Innovative Areas titled “Transcription Cycle” from MEXT; a Grant-in-Aid for Scientific Research (A) from the Japan Society for the Promotion of Science (JSPS); Health Labor Sciences Research Grants (Research on New Drug Development) from the Ministry of Health, Labor and Welfare (MHLW) of Japan; and Research and Development Projects in Cooperation with Academic Institutions from the New Energy and Industrial Technology Development Organization (NEDO) of Japan.

Figure Legends

Figure 1. Salicylic acid binds to FECH and inhibits its enzymatic activity. **(A)** Salicylic acid (SA)-binding proteins were purified from K562 cell lysate with salicylic acid-immobilized (+) or control (–) beads. The indicated concentrations of free salicylic acid were added to the cell lysate before incubation with the beads. Eluted proteins were analyzed by silver staining (top) or immunoblotting (IB, bottom) with anti-FECH antibody. **(B)** Affinity purification was carried out with recombinant FECH R115L. **(C)** Free salicylic acid (SA), *m*-HBA, or *p*-HBA was preincubated with cell lysate derived from FECH R115L-expressing *E. coli* and subjected to affinity purification with salicylic acid-immobilized beads. **(D)** The inhibitory effects of salicylic acid (SA), *m*-HBA, or *p*-HBA on recombinant FECH activity were measured as the percent decrease in the amount of Zn-PpIX produced by aerobic incorporation of zinc into PpIX (n=3; averages and SDs are indicated).

Figure 2. Salicylic acid binds to the dimer interface of FECH. **(A)** Structure of the FECH•SA complex. Two protomers are shown in cyan (chain B) and orange (chain A), respectively, while salicylic acid is colored by elements. **(B)** Close-up view of the salicylic acid-binding region. The Fo-Fc omit map is shown at the 4.0 σ level in green color. Amino acid residues surrounding salicylic acid are shown in the stick model. A hydrogen bond between Ser281 of chain B and the hydroxyl group of salicylic acid is shown with a dotted line. **(C)** Right figure represents a 90° rotation of the FECH•SA structure that is depicted in (B). Left figure shows another possible orientation of SA viewed from the same angle. In both cases, SA forms a hydrogen bond with Ser281 at a distance of 2.7 Å and 2.8 Å. **(D)** FECH R115L and its mutants were expressed in *E. coli*, and their lysates (input) were subjected to affinity purification with control beads (–) or salicylic acid-immobilized (+) beads. Samples were immunoblotted (IB)

with anti-FECH antibody. **(E)** Recombinant GST-tagged human wild-type FECH (hFECH), and *E. coli* FECH (eFECH) were subjected to salicylic acid-binding assays, as in (D). Proteins were visualized by immunoblotting (IB) with an anti-GST antibody. **(F)** Equal amounts of purified recombinant FECH R115L and L311A were incubated with or without the indicated concentrations of salicylic acid for 1 h at 4°C. They were then applied to a Superdex 200 10/300 gel filtration column (GE Healthcare). The same concentrations of salicylic acid were included in the column buffer. Eluate fractions (500 µl each) were collected and analyzed by SDS-PAGE and Coomassie Brilliant Blue staining. Peak positions are shown with down-arrows. The peak positions of gel filtration markers (158, 43, and 13.7 kDa) are shown with up-arrows.

Figure 3. Salicylic acid inhibits heme biosynthesis and mitochondrial activity in K562 cells. **(A)** K562 cells were treated with salicylic acid (SA, red), *m*-HBA (blue), or *p*-HBA (green) for 24 h, extracted, and subjected to UPLC. Heme was detected by measuring the absorbance at 400 nm (n=3; averages and SDs are indicated). The heme content in control K562 cells was set to 100%. **(B)** K562 cells were similarly incubated with the indicated concentrations of SA (red), *m*-HBA (blue), or *p*-HBA (green) for 24 h. WST-8 assays were then performed to measure NAD(P)H content in the cells (n=4; averages and SDs are indicated). The NAD(P)H content in control K562 cells was set to 100%. **(C)** K562 cells were treated with SA (red), *m*-HBA (blue), or *p*-HBA (green) for 24 (left) or 48 h (right) and stained with Rhodamine 123 to measure mitochondrial membrane potential. FCCP (black), a known uncoupler, was used as the positive control.

Figure 4. FECH is responsible for the inhibitory effect of salicylic acid on heme synthesis in 293T cells. **(A)** 293T cells were infected with lentiviral vectors expressing

one of two shRNAs against FECH (FECH sh#1 and FECH sh#2) or a control vector (U6). After selection for a few days, cells were subjected to immunoblot analysis. “293T” represents untransduced 293T cells. **(B)** A fixed number of cells (FECH knockdown cells or control cells) were plated into multiwell plates, treated with the indicated concentrations of salicylic acid (SA) for 24 h, and subjected to UPLC analysis for the quantification of heme. Three independent experiments were performed, and a representative data set is shown.

Figure 5. Salicylic acid inhibits heme synthesis in zebrafish. **(A)** Embryos at 48 hpf were stained with o-dianisidine and inspected under a microscope. Embryos were sorted into “strong,” “intermediate,” and “weak” categories, based on staining intensity and the illustrated diagnostic criteria. **(B)** An AMO against *zFECH* was injected into zebrafish embryos with or without *zFECH* mRNA. Alternatively, embryos were treated with the indicated concentrations of salicylic acid (SA). Shown below the images are the percentages of embryos sorted into “strong,” “intermediate,” and “weak” categories, and the total number of embryos examined for each condition. **(C)** Zebrafish embryos were treated with 0.5 or 1 mM salicylic acid, with or without prior injection of *zFECH* mRNA, and analyzed as in (B). **(D)** Zebrafish embryos were treated with 1 mM salicylic acid (SA), *m*-HBA, or *p*-HBA. They were then processed as in (B). **(E)** Accumulation of PpIX in living 48-hpf embryos was detected by fluorescence microscopy using its autofluorescence with illumination peak at 520-550 nm. Scale bar, 150 μ m. Statistical significance was determined by applying the chi-square contingency test. * $p < 0.05$, *** $p < 0.0001$.

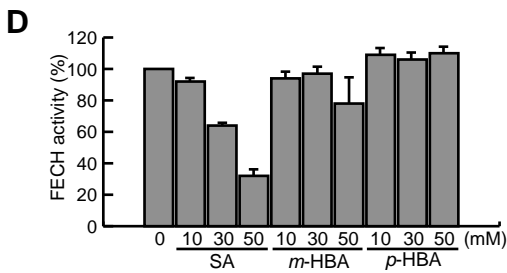
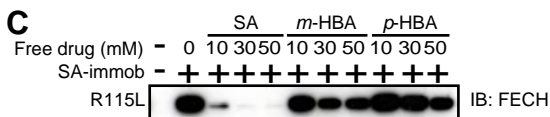
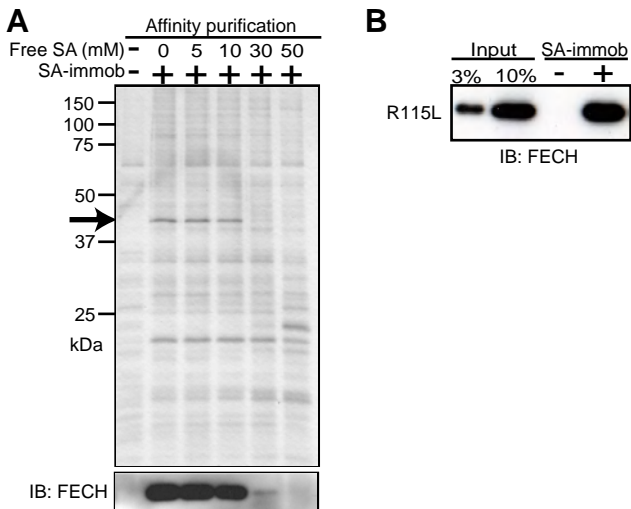
Table 1. Effects of alanine substitutions on FECH activity

Variant	Enzymatic activity ¹	Dimerization status ²	Salicylic acid binding ³
V270A	0%	Monomer	Weak
S281A	~70%	Dimer	Normal
W301A	0%	Monomer	Very weak
L311A	0%	Monomer	Very weak

¹ % of FECH R115L activity, measured as the amount of Zn-PpIX produced.

² Based on gel filtration data.

³ Based on binding assays with salicylic acid-immobilized beads.



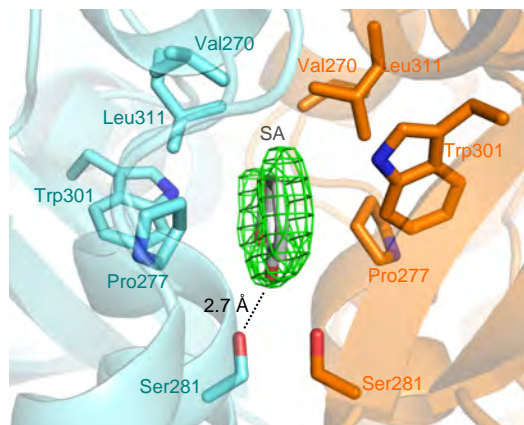
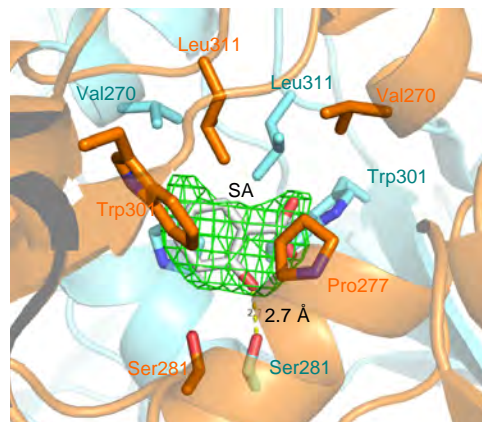
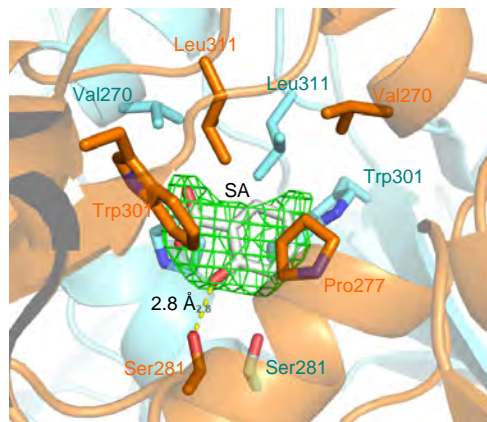
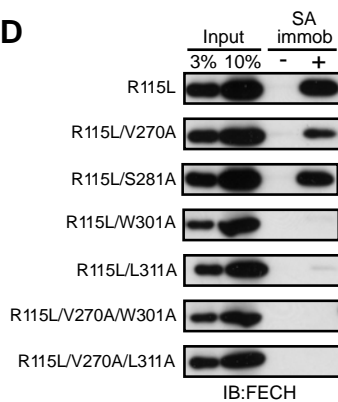
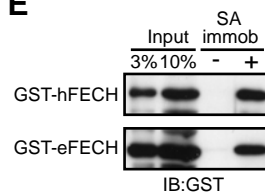
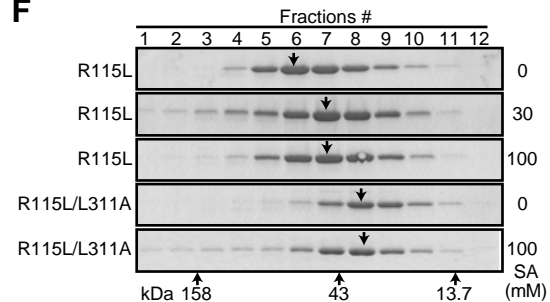
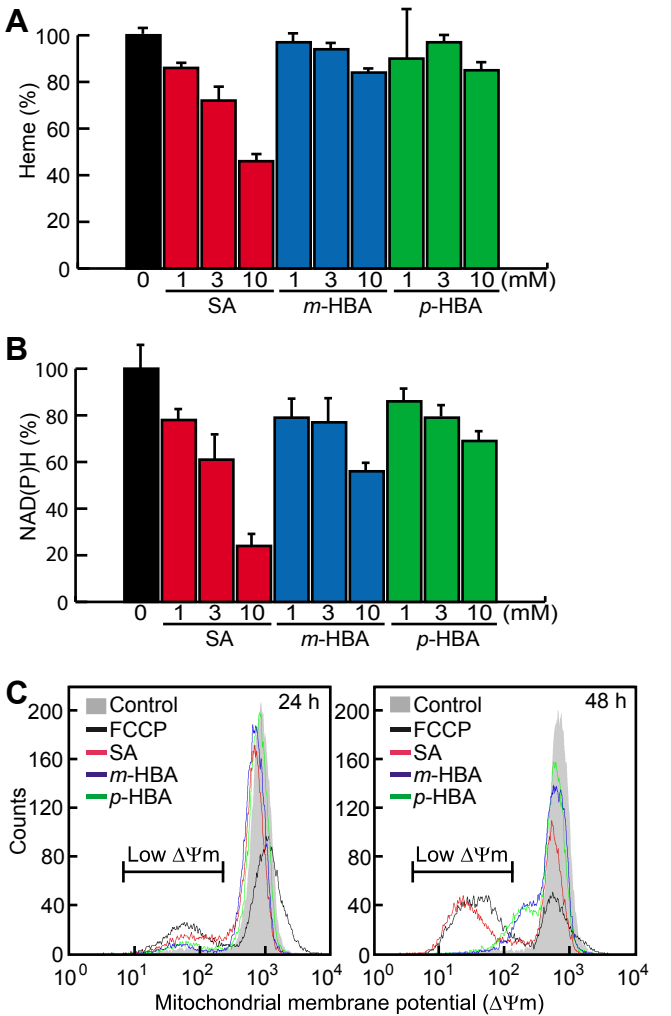
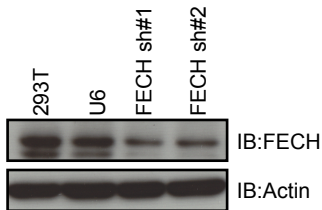
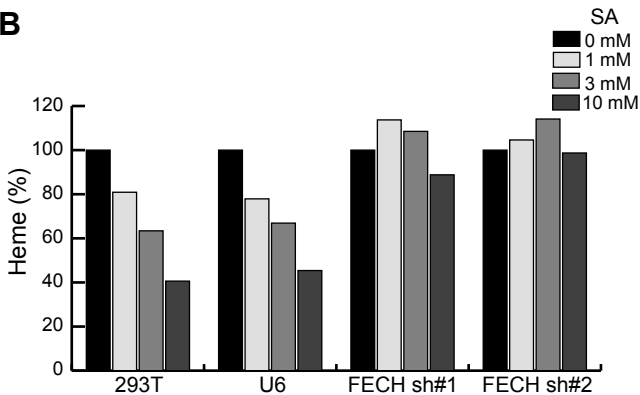
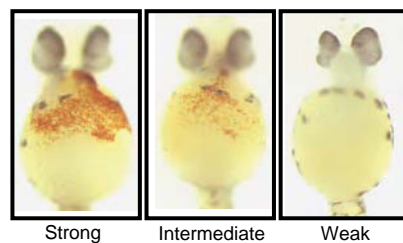
A**B****C****D****E****F**

Figure 3 - 8.9 cm (1 column)

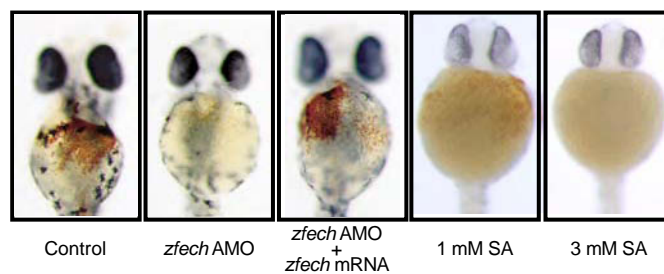


A**B**

A



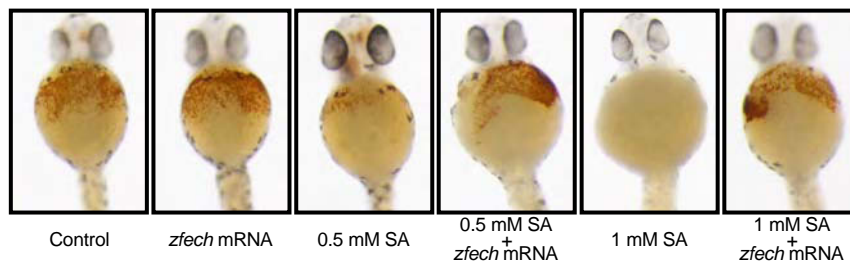
B



# of embryos	82	28	20	83	69
Strong	91%	0%	30%	21%	0%
Intermediate	5%	21%	70%	43%	33%
Weak	4%	79%	0%	36%	67%



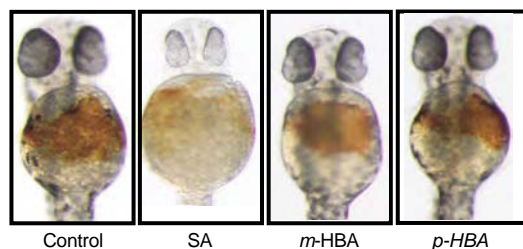
C



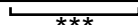
# of embryos	93	32	59	42	82	133
Strong	100%	100%	7%	24%	9%	32%
Intermediate	0%	0%	54%	50%	60%	52%
Weak	0%	0%	39%	26%	31%	16%



D



# of embryos	18	20	20	25
Strong	100%	5%	95%	92%
Intermediate	0%	20%	5%	8%
Weak	0%	75%	0%	0%



E

